Geographic, environmental, and demographic correlates of central nervous system infections in Lao PDR (2003 – 2011): a retrospective secondary spatial analysis

Sayaphet Rattanavong[1], Audrey Dubot-Pérès[1,2,3], Mayfong Mayxay[1,2,4], Manivanh Vongsouvath[1], Sue J Lee[2,5], Julien Cappelle[6,7,8,9], Paul N. Newton[1,2,5], Daniel M. Parker[10,11]

Sayaphet Rattanavong: Sayaphet@tropmedres.ac
Audrey Dubot-Pérès: Audrey@tropmedres.ac
Mayfong Mayxay: Mayfong@tropmedres.ac
Manivanh Vongsouvath: Manivanh@tropmedres.ac
Sue J Lee: Sue@tropmedres.ac
Julien Cappelle: Julien.cappelle@cirad.fr
Paul N. Newton: Paul.Newton@tropmedres.ac
*Daniel M. Parker: Dparker1@uci.edu

*corresponding author

1. Lao-Oxford-Mahosot Hospital-Wellcome Trust Research Unit (LOMWRU), Microbiology Laboratory, Mahosot Hospital, Vientiane, Lao PDR
2. Centre for Tropical Medicine and Global Health, Nuffield Department of Clinical Medicine, University of Oxford, Churchill Hospital, Oxford, U.K.
3. Unité des Virus Émergents (UVE: Aix-Marseille Univ – IRD 190 – Inserm 1207 – IHU Méditerranée Infection), Marseille, France
4. Institute of Research and Education Development, University of Health Sciences, Vientiane, Lao PDR
5. Mahidol-Oxford Tropical Medicine Research Unit, Faculty of Tropical Medicine, Mahidol University, Thailand
6. Epidemiology and Public Health Unit, Institut Pasteur du Cambodge, Phnom Penh, Cambodia.
7. CIRAD, UMR ASTRE, F-34398, Montpellier, France
8. UMR ASTRE, CIRAD, INRA, Montpellier University, F-34398, Montpellier, France.
9. UMR EpiA, INRA, VetAgro Sup, F-69280, Marcy l'Etoile, France.
10. Department of Population Health and Disease Prevention, University of California, Irvine, U.S.A.
11. Department of Epidemiology, School of Medicine, University of California, Irvine, U.S.A.

ABSTRACT

Central nervous system (CNS) infections are important contributors to morbidity and mortality worldwide, but the causative agents for ~50% patients are never identified. Here we present the results of a spatial analysis of CNS infections in Lao PDR (2003 – 2011). Hospitalizations for suspected CNS infection were recorded at Mahosot Hospital in Vientiane and tests for a large panel of pathogens were performed. All home villages were geocoded using patient records and official Lao PDR census data. The spatial distributions of CNS infections were analyzed by major diagnoses. Summary statistics and logistic regressions were used to test for associations between geographic, environmental, and demographic variables and diagnoses. Out of 1,065 patients, 450 (42%) were assigned a confirmed diagnosis. *Japanese encephalitis virus* ((JEV); n=94) and *Cryptococcus* spp. (n=70) were the most common infections. Patients undergoing diagnostic LP for suspected CNS infections lived closer to major roads than would be expected by chance alone. JEV was the most spatially dispersed, peaked in the rainy season and was most common among children. JEV patients came from villages that had higher surface flooding during the same month as admission and, in comparison to the home villages of other patients, came from villages at higher elevation. *Cryptococcus* spp. infections clustered near Vientiane and among adults. Geographic and financial access to healthcare may explain the close proximity of these patients to major roads and also suggest that these hospital data vastly underestimate the true community burden of CNS infections. As Lao PDR is undergoing major developmental and environmental changes, the space-time distributions of the causative agents of CNS infection will also likely change. There is a major need for increased diagnostic abilities; increased access to healthcare, especially for rural populations; and for increased surveillance throughout the nation.

INTRODUCTION

Numerous illnesses go undiagnosed and the causative agents of many infections are never identified. In regions where access to healthcare facilities is limited and where diagnostic capabilities are few, a smaller proportion of diseases are objectively diagnosed. Diseases with mild symptoms may more frequently go untreated, but in some areas even severe illnesses commonly go undiagnosed and untreated. Infections of the central nervous system (CNS) can be particularly severe, affecting the brain and/or spinal cord and/or the surrounding meninges, frequently resulting in death.

Pathogens that invade and infect the CNS include viruses, bacteria, fungi, parasites, and prions. As with other infections, the causative agent(s) of many CNS infections are never determined (frequently <50%) [1–3]. Symptoms of CNS infection can range widely, even for single causative agents, leading to further difficulties with diagnosis. Diagnoses are frequently presumptive and non-specific (i.e. meningitis is often presumed to be caused by bacteria whereas encephalitis is presumed to be caused viruses [2,4–6]). Some causative agents are specific to regions (e.g. Japanese Encephalitis, Saint Louis Encephalitis, Rift Valley Fever Viruses) and exhibit seasonal fluctuations (e.g. vector borne infections), therefore geography and seasonality can facilitate presumptive diagnosis of CNS diseases [4,7].

In Southeast (SE) Asia, CNS infections are increasingly recognized as important contributors to morbidity and mortality [1,8,9]. However, detailed medical and epidemiological data are frequently lacking, especially for low income nations and from remote areas within middle-to-high income nations. Known important viral CNS infections in SE Asia include Japanese encephalitis, dengue, and rabies viruses [1]. Important bacterial CNS infections include *Streptococcus pneumoniae*, *Haemophilus influenzae*, *S. suis*, *Mycobacterium tuberculosis* and

Neisseria meningitidis. *Orientia tsutsugamushi*, *Rickettsia typhi* and *Leptospira* spp. are increasingly recognized as important causes [9]. Detailed analyses that confirm the cause of CNS related infections or assess their spatial and temporal distribution in the region are rare [8–11,14].

We recently published the results of a study of the etiology and impact of CNS infections diagnosed among 1,065 patients at Mahosot Hospital, Vientiane, Lao PDR [14]. The goal of this secondary analysis was to investigate the spatial distribution(s) of CNS-related infections; to look for differential spatial distributions for major causative agents; and to explore potential geographic, demographic, and environmental correlates of these infections.

DATA AND METHODS

Data sources, processing and merging

Data used in this research were compiled from four main sources (**Supporting Figure 1**). The epidemiological data come from an 8-year research project on CNS infections in Lao PDR from all patients who received diagnostic lumbar puncture (LP) at Mahosot Hospital in Vientiane, Lao PDR between January 2003 and August 2011 and consenting to participate [14]. All patients were admitted to the hospital because of suspected CNS infection and Mahosot Hospital is the only medical facility in Lao PDR capable of performing diagnostic LP and cerebral spinal fluid (CSF) analysis. Tests for a large panel of pathogens were performed at the Microbiology Laboratory following international standards (details provided in **Supporting Materials I** and [14]). Demographic (age, gender, ethnicity) and geographic (home village) characteristics of patients were recorded in the database.

The epidemiological data were used to create two separate datasets: One aggregated at the village level (one row per location) and another was maintained at the individual level, with

one row per individual. The official Lao PDR censuses from 2005 and 2015 were used to geocode villages (based on village name and administrative units listed in patient records) and to assign village population estimates to each village (taking a mean population size between 2005 and 2015). Village location and population sizes were then merged to both the individual- and village-level datasets.

A subset of villages within the geographic region of the home villages of included patients was selected by overlaying a standard deviational ellipse with 3 standard deviations (calculations described in **Supporting Materials II**) around the patient home villages and then selecting all villages within that ellipse (**Supporting Figure 2**). These villages were then retained for village level comparisons between villages populated, and not populated, with patients admitted with CNS disease needing an LP. This subset of villages is hereafter referred to as the "study area".

Major road network data was taken from OpenStreetMaps (http://www.openstreetmap.la), selecting "primary", "secondary", and all major connecting roads (downloaded in February 2017, **Supporting Figure 3**). Primary and secondary roads are the two largest road classifications for the nation. Primary roads link major towns and cities and secondary roads link mid-sized towns. Primary and secondary link roads are ramps or slip roads that connect other roads to primary or secondary roads. Together, these types of roads are hereafter referred to as "major roads". Smaller roads were not included in this analysis as they are less likely to be accurately included in the OpenStreetMaps data. The Euclidian distance was then calculated from all villages in the census to the nearest point along a major road. These distances were merged to both the village- and the individual-level datasets.

Environmental predictor variables for vegetation and surface water were derived from Moderate Resolution Imaging Spectroradiometer (MODIS) products (MOD13Q1/MYD13Q1 250 meter AQUA/TERRA 16 day composites). Since many infectious diseases, especially vector borne diseases, are strongly influenced by environmental factors we hypothesized that indicators of vegetation and surface flooding would correlate with some specific diagnoses. Three environmental indices were downloaded and considered in these analyses: a normalized flooding index (NFI) [15]; the normalized difference vegetative index (NDVI); and the enhanced vegetation index (EVI). NFI is indicative of surface water, NDVI is indicative of green surface vegetation, and EVI is an improved measure of green vegetation that is intended to account for dense forest canopies and atmospheric conditions that can lead to error in NDVI measurements. Data were downloaded for each of these environmental indices (EI) within each 16-day time period from February 2002 through December of 2011. The final analyses conducted in this research retained only the EVI and NFI for environmental predictors (summary statistics for NDVI are included) because NDVI and EVI were strongly correlated. The EIs are described in more detail in **Supporting Materials III**.

The environmental raster data were then summarized and extracted based on varying buffer sizes (2km, 5km, and 10km) for each village in the individual- and village-level datasets. Permanent water bodies (such as the Mekong River and Nam Ngum Dam) were masked from the NFI calculations. For the village-level datasets, mean values of each environmental variable was calculated for the study period duration and used as an indicator of “average” vegetation or surface water characteristics of each village. For the individual-level dataset the values were extracted based on the admission date, using increasing durations of time prior to admission (within the same month, within the previous 2 months, within the previous year).

The final datasets include the village-level data, that is a subsample of 98% of all villages with patients included in the study and the other census designated villages within the same region (the study area), and the individual level dataset that includes all patients included in the study. Variables used in this analysis and their descriptions are listed in **Table 1**.

Exploratory spatial data analysis

Summary statistics (median; Q1:Q3; mean) were calculated for the distances between villages and the nearest major road, and aggregated by whether or not the village was home to included patients and by specific diagnoses. Summary statistics (mean and 95% confidence intervals) were also calculated for all environmental variables, at each buffer size and temporal resolution, and for each of the major diagnoses. Tukey's post hoc range test was used to assess statistically significant differences in environmental indices across diagnoses.

Standard distance deviations (SDDs) and standard deviation ellipses (SDEs) were calculated (**details in Supporting Materials II**) and mapped to measure and visually analyze the central tendency and spatial distributions for all patient home villages and by each of the major single (mono-infection) diagnoses.

Formal analyses

Multivariable regressions were used to calculate model-adjusted odds ratios and confidence intervals. The regressions at the village level focused on study patient villages and the home villages of JEV diagnosed patients. A multivariable regression was also done at the individual level focusing on JEV infected patients. Other diagnoses were not included in these analyses because of small numbers of cases per village.

Logistic generalized additive models (GAMs) were used for variable selection and specification (**detailed in Supporting Materials IV and in Table 1**) for the final models. The

GAMs were used to examine different specifications of the continuous environmental, geographic, and demographic variables and for changes in model fit and strength of association across buffer sizes (i.e. 2km, 5km, or 10km buffers) and for different time durations for EI measurements (i.e. same month, 2 months prior, 12 months prior to hospital admission). The final model covariates were chosen based on a combination of *a priori* hypotheses, model fit (using the Akaike information criterion), and strength of association between the covariate and the model outcome variable.

The final model for the individual-level analysis was a generalized logistic mixed model with a random effect for home village. The final model for the village-level analysis was a logistic regression.

Software

All maps were created using QGIS version 3.4.9. R cran version 3.5.2 was used for downloading, processing, and wrangling MODIS data (using the "MODIStsp"; "raster"; "rgdal"; and "maptools" packages) and for all regressions. The "mgcv" package was used for GAMs and the lme4 package was used for the generalized mixed models. Euclidian distances between villages and major roads were calculated using QGIS. ArcMap version 10.5.1 was used to calculate SDDs and SDEs.

Ethics approval

Ethical clearance for the CNS study was granted by the Oxford University Tropical Ethics Research Committee and by the Ethical Review Committee of the Faculty of Medical Sciences, National University of Laos. Verbal consent (from 2003 – 2006) and written consent (from 2006 – 2011) were obtained from all recruited patients or immediate relatives.

RESULTS

Summary statistics

A total of 1,065 patients were recruited with no LP contraindications and consented to have a diagnostic LP; 450 (42%) were assigned a final laboratory diagnosis. The most common of these were *Japanese encephalitis virus* ((JEV) 94 individuals); followed by *Cryptococcus* spp. with 70 individuals (9 were *C. gattii*)); scrub typhus (*Orientia tsutsugamushi*) 31; *Dengue virus* 27; *Leptospira* spp. 25; murine typhus (*Rickettsia typhi*) 24; *Streptococcus pneumoniae* in 22 and 20 with *Mycobacterium tuberculosis*. 124 patients died prior to discharge (out of 893 with recorded discharge type recorded).

The majority (666, 63%) of patients were male, with the lowest sex bias in cryptococcal infections (40/70, 57% male) and the highest among dengue infections (22/27, 82% male) (**Table 2**). Age patterns were evident in JEV and cryptococcal infections, with median ages of 13 and 33 years, respectively (**Table 2**). Patients were linked to 582 different villages (multiple patients could come from the same village): 90 villages with JEV patients, 66 with cryptococcal patients, 31 with scrub typhus patients, 27 with dengue patients, 24 with leptospiral patients, and 24 with murine typhus patients. The majority (870, 82%) of patients came from within Vientiane Prefecture (678, 64%) or Vientiane Province (192, 18%).

A total of 6,416 villages (of 10,520 recorded in 2005 [16]) were selected as the study area for further village level analyses (**Table 3**). Villages that were home to study patients were 11 times (0.7km versus 6.3km, from **Table 3**) closer to a major road when compared to other villages within the study area. Scrub typhus and JEV infected patient homes were further from major roads than other patients, but the difference was not statistically significant in univariate analyses.

The home villages of JEV patients were more broadly dispersed (**Figure 1B**) than for patients with other etiologies (**Figure 1C**), evident from the circular, larger SDE and SDD. The distribution of these JEV patient home villages was also relatively isotropic, with the SDE and SDD being nearly identical. Conversely, patients with cryptococcal infections were clustered near Vientiane City and along the road leading North/Northwest from the urban center (**Figure 1C**). Scrub typhus and murine typhus infections were also both clustered around Vientiane City but showed perpendicular spatial distributions (**Supporting Figures 4D and 4G**) a pattern previously described from IgG seropositivity data from Vientiane City [17]).

Characteristics of patient home villages

Mean NFI values for the 2km radius tended to be higher than for either the 5km or 10km radius as surface flooding is heterogeneous and taking a mean across larger radii dilutes the measurement. The opposite pattern was observed for both vegetation indices. The 2km radius for both mean NDVI and mean EVI was usually smaller than at 5km or 10km radii (**Figures 2 and 3**).

Study patient villages had higher mean NFI values than non-study patient villages (**Figure 2A**) (non-study patient villages are those in the same study area as study patient villages but were not home to a study patient). The home villages of study patients diagnosed with *dengue virus* and cryptococcal infections had high mean NFI values over the duration of the study period when compared to other major diagnoses (**Figure 2A**).

Conversely, the home villages of study patients tended to have lower mean EVI values than non-study patient villages (**Figure 2C**). Villages from which patients who were diagnosed with JEV were an exception to this general pattern. JEV patient home villages had higher mean

EVI when compared to home villages of patients with dengue and cryptococcal infections (**Figure 2C**).

Home villages of patients with JEV diagnoses had lower mean NFI over the duration of the study period, but had higher NFI than other major diagnoses when looking specifically at the month of admission (especially when compared to cryptococcal infections and murine typhus (**Figure 3A**)). JEV patient home villages also had higher EVI during the month of admission than most other mono-infections, especially when compared to either cryptococcal infections or murine typhus (**Figure 3C**). Scrub typhus infections had higher EVI than cryptococcal infections when the measurement was taken at the 10km radius buffer (not detectable at smaller radii (**Figure 3C**)).

Home villages of patients with dengue infections had higher NFI than murine typhus or *Cryptococcus* spp. patient home villages when considering the 2 months prior to admission (**Figure 3D**). *Cryptococcus* spp. patient home villages had particularly low EVI in the two months leading up to admission, especially when compared to JEV and *Leptospira* spp. patient home villages (**Figure 3F**).

At one year prior to admission both *Cryptococcus* spp. patient home and *dengue virus* patient home villages had higher NFI than JEV patient home villages (**Figure 3G**).

Logistic regressions for geographic, environmental and demographic predictors of CNS infections

In agreement with univariate analyses, villages from which study patients came tended to be larger in population size (**Supporting Figure 4**), lower in elevation (**Supporting Figure 5**), and closer to a major road when compared to other villages within the study area (**Table 4**). They also had higher mean levels of surface flooding, with villages in the highest NFI quadrant having

over two times the odds (AOR: 2.21; CI: 1.49 – 3.31) of being a home village for study patients when compared to neighboring villages in the study area (**Table 4 and Figure 2**). Villages from which JEV patients originated had few defining characteristics in the logistic regression, other than being larger in population size (AOR: 1.74; CI: 1.55 – 1.96) and at lower elevations (AOR: 0.69; CI: 0.46 – 0.97) than non-study patient villages (**Table 5**).

In the individual-level analysis (**Table 6**), age and season were the strongest predictors of JEV infections among all patients. Patients who were admitted between July and September had over seven times the odds (AOR: 7.40; CI: 1.45 – 37.67) of being diagnosed with JEV when compared to patients who were admitted between January and March (**Table 6**). JEV was most common in children aged 5 through 14 (AOR: 2.74; CI: 1.31 – 5.69; ages 0 – 4 as the comparison group). NFI during the month of admission (10km buffer used in the regression) was also a strong predictor of JEV infection. Individuals who came from villages in the highest quadrant of NFI measurements had approximately 3 times the odds being diagnosed with JEV (AOR: 3.06; CI: 1.04 – 8.96). While study patients came from villages with lower mean elevations, patients who were diagnosed with JEV came from higher elevation villages in comparison to the other patients (AOR: 1.36; CI: 1.11 – 1.66). EVI was a significant predictor in models that did not include distance to road, village population, and elevation (**Table 6 M1 and M2**).

DISCUSSION

Patients from this study were recruited based on symptomology and a medical procedure that is only available at a single location in the nation (diagnostic LP at Mahosot Hospital, Vientiane). The home villages of all included study patients, regardless of diagnosis, were

298 approximately centered on Vientiane City and were closer to major roads than would be
299 expected by chance alone. For many of the infections studied in this analysis, this association is
300 likely more related to geographic and financial access to healthcare systems rather than exposure
301 to environmental risk factors – especially for infections that are more associated with rural areas
302 (e.g. JEV). This finding also suggests that the results here may be a vast underestimate of the true
303 burden of CNS infections, with much of the Lao population not being in near proximity to a
304 major road (**Table 3**). The causative agents of CNS infections differ in biology, ecology, and
305 geography, and this is evident through the spatial distributions of the home villages of patients.
306 The geographic, environmental, and demographic patterns exhibited by patients needing a
307 diagnostic LP for suspected CNS infections, and for specific diagnoses, are the result of complex
308 overlapping factors.

309 A similar spatial pattern was described from an epidemiological analysis of CNS
310 infections among children admitted to Ho Chi Minh City hospitals in Vietnam – with most
311 patients coming from districts near the hospital [12]. While the majority of infections (55%) in
312 the Vietnam study were presumed to be bacterial in origin, in this study from Lao PDR bacterial
313 infections were identified in only 38% (170 out of 450 patients with diagnoses).

314 JEV was the single largest identified cause of CNS infections in these data; it primarily
315 affected children (median 13 years of age, **Table 2**), occurred predominantly during the rainy
316 season (likely corresponding to peaks in mosquito vector populations), and in villages with
317 recent high levels of surface water [18]. JEV is a vaccine-preventable disease, but the vaccine
318 has historically been expensive and vaccine programs are frequently limited by access to remote
319 communities. In 2013 the WHO approved a less expensive vaccine (produced in China by the
320 Chengdu Institute of Biological Products) which has since been used in mass vaccination

campaigns in Lao PDR in 2013 and 2015 [19]. The vaccine is now routinely given to all children less than 9 months of age but coverage may be low in some areas.

The second largest contributor to CNS diseases were cryptococcal infections, which are opportunistic fungal infections with high mortality [20]. Of the 70 patients with cryptococcal infections, 12 died prior to discharge and another 8 likely died at home after leaving the hospital. Cryptococcal infections are generally acquired after inhalation of the yeast-like form of the fungus which has been associated with several ecological habitats (*Cryptococcus gattii* has been associated with over 50 species of trees; *Cryptococcus neoformans* has been associated with bird droppings but is also suspected to be associated with plants [21,22]). This disease has a long incubation period [23,24] and while *C. gattii* infections commonly occur among immunocompetent individuals, *C. neoformans* infections are frequently associated with HIV infections [25,26]. In these data, 20 of the patients diagnosed with cryptococcal infections also had HIV infections. While several studies have shown that cryptococcal species exist in specific ecological habitats and have inferred environmental exposure, the long incubation period and complex natural history likely obfuscate ecological correlations.

There are several limitations to this research. Diagnostic LPs are only conducted in Mahosot Hospital in the national capital. Logistical and financial difficulties in accessing healthcare facilities, and especially for etiological diagnostic capabilities, likely leads to severe under-reporting of meningitis, encephalitis, or in the diagnosing the causative agent in these conditions when the patient does access care. All of these factors ultimately lead to small case counts for numerous different causative agents. The spatial patterns in points (villages) and ellipses exhibited in these data are likely influenced by the shape of the nation and it is possible that the point patterns and ellipses would differ if we had data from neighboring nations. Spatial

and temporal patterns that differentiate different infections might be more obvious if the surveillance system instead focused on any symptomatic infections (rather than only suspected infections of the CNS). Some pathogens are neurotropic whereas others have tropism for other organs, while being capable of occasionally infecting the CNS. This may partially explain the higher case counts of JEV and why we were able to identify spatial, temporal, and environmental predictors for this causative agent.

OpenStreetMaps data are volunteered data and may be prone to error. For this reason we focused on major roads, whose routes have changed very little over the last decades. For the regressions, the distances from all villages to the nearest major road was also rounded to the nearest 5km. Examination of satellite imagery in comparison with the major roads from OpenStreetMaps suggests that where error does exist, it is on a scale of $\pm$100 meters, meaning that measurements of distances, as used in this analysis, should not be strongly influenced. Some of these data now come from over a decade ago. Surveillance systems of this type (based on relatively vague symptomology), with a wide panel of possible contributing causative agents, and necessary intensive laboratory components are extremely labor and time intensive.

Lao PDR is currently undergoing vast environmental, demographic, and economic changes. Road networks are increasing in range and density and several areas (i.e. Vientiane, Savannakhet) are undergoing expansive urbanization [27]. These environmental changes will most likely result in shifting patterns of infectious diseases. As the region undergoes urbanization (including both a decrease in urban landscape and movement of human populations to urban centers), pathogens that thrive in rural areas (e.g. JEV) may undergo reduced transmission, especially if vaccine campaigns are more capable of reaching rural populations. Conversely,

infections that cluster in urban and peri-urban areas (such as dengue and murine typhus) may increase in frequency.

Several environmental indices from remote sensing instruments have shown potential for predicting disease risk, differentiating disease types, or for other surveillance efforts in SE Asia [28,29] and globally [30–34]. This analysis, and others like it, illustrates the ability to differentiate some infections (namely JEV when compared to other diagnoses) through the use of freely available data (i.e. MODIS) and software (R and QGIS) and routinely collected healthcare data. Surveillance systems and potentially diagnostic algorithms [35] in developing settings could benefit from inclusion of such resources. A far-reaching surveillance system that is representative of the entire nation and includes likely CNS infections would be beneficial in order to assess the true burden of CNS infections – many of which would benefit from primary and secondary prevention through increased provision of vaccines, vector control, and early diagnosis and treatment. Given the inherent difficulties in accurately diagnosing and treating CNS infections, the predictors reported here and from other epidemiological studies for major contributors to CNS diseases (i.e. age, seasonality, location, and environmental characteristics) could be considered alongside clinical symptomology when presumptive diagnoses are being made. However, it will be important to consider current and ongoing demographic, environmental, and economic changes in Lao PDR.

Finally, increasing population access to vaccines, diagnosis, and treatment would have clear benefits to overall population health. As with other parts of the developing world, a large fraction of the Lao population must travel long distances in order to reach primary healthcare centers. In 2005 73% of the Lao population was reported to live in rural areas, 21% without roads. By 2015 67% of the population were reported to live in rural villages with 8% in villages

without roads [36]. For many communities, travel during the wet season remains difficult. Travel costs can also be prohibitive. Most of the CNS infections in this analysis occurred or developed symptoms during the wet season. Public health initiatives that help to decrease the distances between communities and the healthcare services that they need are warranted.

Acknowledgements

We are very grateful to the patients and to Bounthaphany Bounxouei, past Director of Mahosot Hospital; to Bounnack Saysanasongkham, Director of Department of Health Care, Ministry of Health; to H.E. Bounkong Syhavong, Minister of Health, Lao PDR; to the staff of the Infectious Disease Center and Microbiology Laboratory for their help and support.

Funding

This study was supported by the European Commission Innovate program (ComAcross project, grant no. DCI-ASIE/2013/315-047). The work of LOMWRU, PN and MM are funded by the Wellcome Trust of Great Britain, grant 106698/Z/14/Z. Travel to Lao PDR to support DMP for this research was obtained through a University of California Council on Research, Computing, and Libraries (CORCL) Faculty Grant.

REFERENCES

1. Tarantola A, Goutard F, Newton P, de Lamballerie X, Lortholary O, Cappelle J, et al. Estimating the Burden of Japanese Encephalitis Virus and Other Encephalitides in Countries of the Mekong Region. PLoS Neglected Tropical Diseases. 2014;8: 4. doi:10.1371/journal.pntd.0002533

2. Glaser C a, Honarmand S, Anderson LJ, Schnurr DP, Forghani B, Cossen CK, et al. Beyond viruses: clinical profiles and etiologies associated with encephalitis. Clinical infectious diseases : an official publication of the Infectious Diseases Society of America. 2006;43: 1565–1577. doi:10.1086/509330

3. Glaser CA, Gilliam S, Schnurr D, Forghani B, Honarmand S, Khetsuriani N, et al. In Search of Encephalitis Etiologies: Diagnostic Challenges in the California Encephalitis Project, 1998–2000. Clinical Infectious Diseases. 2003;36: 731–742. doi:10.1086/367841

4. Solomon T, Michael BD, Smith PE, Sanderson F, Davies NWS, Hart IJ, et al. Management of suspected viral encephalitis in adults – Association of British Neurologists and British Infection Association National Guidelines. Journal of Infection. 2012;64: 347–373. doi:10.1016/j.jinf.2011.11.014

5. McGill F, Heyderman RS, Michael BD, Defres S, Beeching NJ, Borrow R, et al. The UK joint specialist societies guideline on the diagnosis and management of acute meningitis and meningococcal sepsis in immunocompetent adults. Journal of Infection. 2016;72: 405–438. doi:10.1016/j.jinf.2016.01.007

6. Bharucha T, Vickers S, Ming D, Lee SJ, Dubot-Pérès A, de Lamballerie X, et al. Association between reported aetiology of central nervous system infections and the speciality of study investigators—a bias compartmental syndrome? Trans R Soc Trop Med Hyg. 2017;111: 579–583. doi:10.1093/trstmh/try008

7. Kennedy PGE. Viral Encephalitis: Causes, Differential Diagnosis, and Management. Journal of Neurology, Neurosurgery & Psychiatry. 2004;75: i10–i15. doi:10.1136/jnnp.2003.034280

8. Olsen SJ, Campbell AP, Supawat K, Liamsuwan S, Chotpitayasunondh T, Laptikulthum S, et al. Infectious Causes of Encephalitis and Meningoencephalitis. 2015;21: 2003–2005.

9. Dittrich S, Rattanavong S, Lee SJ, Panyanivong P, Craig SB, Tulsiani SM, et al. Orientia, rickettsia, and leptospira pathogens as causes of CNS infections in Laos: A prospective study. The Lancet Global Health. 2015;3: e104–e112. doi:10.1016/S2214-109X(14)70289-X

10. Mai NTH, Phu NH, Nhu LNT, Hong NTT, Hanh NHH, Nguyet LA, et al. Central Nervous System Infection Diagnosis by Next-Generation Sequencing: A Glimpse Into the Future? Open Forum Infect Dis. 2017;4. doi:10.1093/ofid/ofx046

11. Turner P, Suy K, Tan LV, Sar P, Miliya T, Hong NTT, et al. The aetiologies of central nervous system infections in hospitalised Cambodian children. BMC Infect Dis. 2017;17. doi:10.1186/s12879-017-2915-6

12. Ho NT, Hoang VMT, Le NNT, Nguyen DT, Tran A, Kaki D, et al. A spatial and temporal analysis of paediatric central nervous system infections from 2005 to 2015 in Ho Chi Minh City, Vietnam. Epidemiology and Infection. 2017;145: 3307–3317. doi:10.1017/S095026881700228X

13. Mawuntu AHP, Bernadus JBB, Dhenni R, Wiyatno A, Anggreani R, Feliana, et al. Detection of central nervous system viral infections in adults in Manado, North Sulawesi, Indonesia. PLOS ONE. 2018;13: e0207440. doi:10.1371/journal.pone.0207440

14. Dubot-Pérès A, Mayxay M, Phetsouvanh R, Lee SJ, Rattanavong S, Vongsouvath M, et al. Management of Central Nervous System Infections, Vientiane, Laos, 2003–2011 - Volume 25, Number 5—May 2019 - Emerging Infectious Diseases journal - CDC. doi:10.3201/eid2505.180914

15. Boschetti M, Nutini F, Manfron G, Brivio PA, Nelson A. Comparative analysis of normalised difference spectral indices derived from MODIS for detecting surface water in flooded rice cropping systems. PLoS ONE. 2014;9. doi:10.1371/journal.pone.0088741

16. Lao Population and Housing Census 2015: Provisional Report [Internet]. Ministry of Planning and Investment Lao Statistics Bureau; 2015 Dec p. 64. Available: https://lao.unfpa.org/sites/default/files/pub-pdf/Final%20report-editting-English1.pdf

17. Vallé J, Thaojaikong T, Moore CE, Phetsouvanh R, Richards AL, Souris M, et al. Contrasting spatial distribution and risk factors for past infection with scrub typhus and murine typhus in Vientiane city, Lao PDR. PLoS Neglected Tropical Diseases. 2010;4: 1–10. doi:10.1371/journal.pntd.0000909

18. Campbell G, Hills S, Fischer M, Jacobson J, Hoke C, Hombach J, et al. Estimated global incidence of Japanese encephalitis: Bulletin of the World Health Organization. 2011;89: 766–774. doi:10.2471/BLT.10.085233

19. UNICEF. Japanese Encephalitis Vaccine Market and Supply Update. 2015;

20. Slavin MA, Chakrabarti A. Opportunistic fungal infections in the Asia-Pacific region. Medical Mycology. 2012;50: 18–25. doi:10.3109/13693786.2011.602989

21. Springer DJ, Chaturvedi V. Projecting global occurrence of Cryptococcus gattii. Emerging Infectious Diseases. 2010;16: 14–20. doi:10.3201/eid1601.090369

22. Ellis DH, Pfeiffer TJ. Ecology, life cycle, and infectious propagule of Cryptococcus neoformans. The Lancet. 1990;336: 923–925. doi:10.1016/0140-6736(90)92283-N

23. Castrodale LJ, Gerlach RF, Preziosi DE, Frederickson P, Lockhart SR. Prolonged incubation period for cryptococcus gattii infection in cat, Alaska, USA. Emerging Infectious Diseases. 2013;19: 1034–1035. doi:10.3201/eid1906.130006

24. Georgi A, Schneemann M, Tintelnot K, Calligaris-Maibach RC, Meyer S, Weber R, et al. Cryptococcus gattii meningoencephalitis in an immunocompetent person 13 months after exposure. Infection. 2009;37: 370–373. doi:10.1007/s15010-008-8211-z

25. Wright P, Inverarity D. Human immunodeficiency virus (HIV) related cryptococcol meningitis in rural Central Thailand-Treatment difficulties and prevention strategies. Southeast Asian J Trop Med Public Health. 2007;38: 4.

26. Inverarity D, Bradshaw Q, Wright P, Grant A. The spectrum of HIV-related disease in rural Central Thailand. Southeast Asian J Trop Med Public Health. 2002;33: 10.

27. Bank AD. Urban development in the Greater Mekong Subregion. Steinberg F, Hakim J, editors. Mandaluyong City, Philippines: Asian Development Bank; 2016. doi:10.1111/j.1467-9787.2010.00709.x

28. Ledien J, Sorn S, Hem S, Huy R, Buchy P, Tarantola A, et al. Assessing the performance of remotely-sensed flooding indicators and their potential contribution to early warning for leptospirosis in Cambodia. Schumann GJ-P, editor. PLOS ONE. 2017;12: e0181044. doi:10.1371/journal.pone.0181044

29. Chadsuthi S, Chalvet-Monfray K, Wiratsudakul A, Suwancharoen D, Cappelle J. A remotely sensed flooding indicator associated with cattle and buffalo leptospirosis cases in Thailand 2011–2013. BMC Infectious Diseases. 2018;18. doi:10.1186/s12879-018-3537-3

30. Rogers DJ, Randolph SE, Snow RW, Hay SI. Satellite imagery in the study and forecast of malaria. Nature. 2002;415: 710–715. doi:10.1038/415710a

31. Lambin EF, Tran A, Vanwambeke SO, Linard C, Soti V. Pathogenic landscapes: Interactions between land, people, disease vectors, and their animal hosts. International Journal of Health Geographics. 2010;9: 54. doi:10.1186/1476-072X-9-54

32. Beck LR, Lobitz BM, Wood BL. Remote sensing and human health: new sensors and new opportunities. Emerg Infect Dis. 2000;6: 217–227.

33. Ford TE, Colwell RR, Rose JB, Morse SS, Rogers DJ, Yates TL. Using Satellite Images of Environmental Changes to Predict Infectious Disease Outbreaks. Emerg Infect Dis. 2009;15: 1341–1346. doi:10.3201/eid/1509.081334

34. Lleo MM, Lafaye M, Guell A. Application of space technologies to the surveillance and modelling of waterborne diseases. Curr Opin Biotechnol. 2008;19: 307–312. doi:10.1016/j.copbio.2008.04.001

35. Pokharel S, White LJ, Aguas R, Celhay O, Pellé KG, Dittrich S. Algorithm in the diagnosis of febrile illness using pathogen-specific rapid diagnostic tests. Clin Infect Dis. doi:10.1093/cid/ciz665

36. Results of the Population and Housing Census 2015 [Internet]. Lao Statistics Bureau; 2016 p. 282. Available: https://lao.unfpa.org/sites/default/files/pub-pdf/PHC-ENG-FNAL-WEB_0.pdf

37. Leparc-Goffart I, Baragatti M, Temmam S, Tuiskunen A, Moureau G, Charrel R, et al. Development and validation of real-time one-step reverse transcription-PCR for the detection and typing of dengue viruses. J Clin Virol. 2009;45: 61–66. doi:10.1016/j.jcv.2009.02.010

38. Moureau G, Temmam S, Gonzalez JP, Charrel RN, Grard G, de Lamballerie X. A real-time RT-PCR method for the universal detection and identification of flaviviruses. Vector Borne Zoonotic Dis. 2007;7: 467–477. doi:10.1089/vbz.2007.0206

523 39. Moureau G, Ninove L, Izri A, Cook S, De Lamballerie X, Charrel RN. Flavivirus RNA in
524 phlebotomine sandflies. Vector Borne Zoonotic Dis. 2010;10: 195–197.
525 doi:10.1089/vbz.2008.0216

526 40. Jiang J, Chan T-C, Temenak JJ, Dasch GA, Ching W-M, Richards AL. Development of a
527 quantitative real-time polymerase chain reaction assay specific for Orientia tsutsugamushi.
528 Am J Trop Med Hyg. 2004;70: 351–356.

529 41. Jiang J, Stromdahl EY, Richards AL. Detection of Rickettsia parkeri and Candidatus
530 Rickettsia andeanae in Amblyomma maculatum Gulf Coast Ticks Collected from Humans
531 in the United States. Vector-Borne and Zoonotic Diseases. 2011;12: 175–182.
532 doi:10.1089/vbz.2011.0614

533 42. Phetsouvanh R, Blacksell SD, Jenjaroen K, Day NPJ, Newton PN. Comparison of Indirect
534 Immunofluorescence Assays for Diagnosis of Scrub Typhus and Murine Typhus Using
535 Venous Blood and Finger Prick Filter Paper Blood Spots. The American Journal of
536 Tropical Medicine and Hygiene. 2009;80: 837–840. doi:10.4269/ajtmh.2009.80.837

537 43. Thaipadunpanit J, Chierakul W, Wuthiekanun V, Limmathurotsakul D, Amornchai P,
538 Boonslip S, et al. Diagnostic Accuracy of Real-Time PCR Assays Targeting 16S rRNA and
539 lipl32 Genes for Human Leptospirosis in Thailand: A Case-Control Study. PLOS ONE.
540 2011;6: e16236. doi:10.1371/journal.pone.0016236

541 44. Cole JR, Sulzer CR, Pursell AR. Improved Microtechnique for the Leptospiral Microscopic
542 Agglutination Test1. Appl Microbiol. 1973;25: 976–980.

543 45. Mitchell A. The ESRI Guide to GIS Analysis. ESRI Press; 2005.

544 46. Levine N. Spatial Distribution. CrimeStat III: a spatial statistics program for the analysis of
545 crime incident locations (version 30). Houston, TX; Washington DC: Ned Levine &
546 Associates; National Institute of Justice; 2004. Available:
547 https://www.nij.gov/topics/technology/maps/documents/crimestat-
548 files/CrimeStat%20IV%20Chapter%204.pdf

549 47. Rouse J, Hass R, Deering D, Sehell J. Monitoring the vernal advancement and
550 retrogradation (Green wave effect) of natural vegetation [Internet]. 1974 p. 8. Report No.:
551 E74-10676, NASA-CR-139243, PR-7. Available:
552 https://ntrs.nasa.gov/archive/nasa/casi.ntrs.nasa.gov/19740022555.pdf

553 48. Huete AR. A soil-adjusted vegetation index (SAVI). Remote Sensing of Environment.
554 1988;25: 295–309. doi:10.1016/0034-4257(88)90106-X

555 49. Huete A, Didan K, Miura T, Rodriguez E, Gao X, Ferreira L. Overview of the radiometric
556 and biophysical performance of the MODIS vegetation indices. Remote Sensing of
557 Environment. 2002;83: 195–213. doi:10.1016/S0034-4257(02)00096-2

558 50. Hale GM, Querry MR. Optical Constants of Water in the 200-nm to 200-μm Wavelength
559 Region. Appl Opt, AO. 1973;12: 555–563. doi:10.1364/AO.12.000555

51. Boschetti M, Nutini F, Manfron G, Brivio PA, Nelson A. Comparative Analysis of Normalised Difference Spectral Indices Derived from MODIS for Detecting Surface Water in Flooded Rice Cropping Systems. Schumann GJ-P, editor. PLoS ONE. 2014;9: e88741. doi:10.1371/journal.pone.0088741

586 **Table 1:** List of variables, their spatial and temporal scales, and transformations

587

Variable	description	spatial scale	temporal scale	transformation
Village population	Population estimate of LP patient home village. This is calculated as a mean population value from the Lao PDR official census from years 2005 and 2015.			For multivariable regressions, this variable was centered on its mean and standardized by its standard deviation
Distance to major road	This is the distance in meters from the LP patient home village and the nearest point on a major highway network, from the OpenStreetMaps map layer. This distance was transformed into kilometers and rounded to the nearest 5 kilometers in order to account for measurement error.	This distance was transformed into kilometers and rounded to the nearest 5 kilometers in order to account for measurement error.		For multivariable regressions, this variable was centered on its mean and standardized by its standard deviation.
Village elevation	This is the elevation of the LP patient home village, calculated from a digital elevation model. It is in meters above sea level.	at village point		For multivariable regressions, this variable was centered on its mean and standardized by its standard deviation
NFI	This is the normalized flooding index, described in detail in the Supporting materials.	Mean values at 2km, 5km, and 10km buffers around each village.	For village level analysis: calculated as a mean value for the study duration. For individual level analysis: Calculated for the same month (same 16 day time period); the previous 2 months (mean of the previous 5 16 day intervals); and the previous year (mean of the previous 23 16 day intervals).	Aggregated into quartiles for multivariable regressions.
NDVI	This is the normalized difference vegetation index, detailed in the Supporting materials.	Mean values at 2km, 5km, and 10km buffers around each village.	For village level analysis: calculated as a mean value for the study duration. For individual level analysis: Calculated for the same month (same 16 day time period); the previous 2 months (mean of the previous 5 16 day intervals); and the previous year (mean of the previous 23 16 day intervals).	
EVI	This is the enhanced vegetation index, detailed in the Supporting materials.	Mean values at 2km, 5km, and 10km buffers around each village.	For village level analysis: calculated as a mean value for the study duration. For individual level analysis: Calculated for the same month (same 16 day time period); the previous 2 months (mean of the previous 5 16 day intervals); and the previous year (mean of the previous 23 16 day intervals).	Aggregated into quartiles for multivariable regressions.
Gender	Binary for male or female, self reported in hospital records			
Age	Self reported age in years.			Aggregated into age groups for multivariable
Year	The year of admission to the hospital			For multivariable regressions, this variable was centered on its mean and standardized by its standard deviation.
Quarter	The calendar quarter of admission (Jan - March; Apri - June; July - Sep; Oct - Dec)			

588

589

590

591

592

593

594

595

Table 2: Age and gender of study patients. (Q1 and Q3 indicate the first and third quartiles, respectively).

	male/female	M/F ratio	median age in years (Q1 –Q3)	Total number
all patients	666/399	1.67	23 (8 - 38)	1065
JEV	55/39	1.41	13 (8 - 20)	94
***Cryptococcus* spp.**	40/30	1.33	33 (27 - 41)	70
scrub typhus	22/9	2.44	16 (9 - 29)	31
Dengue virus	22/5	4.4	20 (9 - 30)	27
***Leptospirosis* spp.**	17/8	2.13	25 (12 - 39)	25
murine typhus	17/7	2.43	32 (16 - 51)	24

Table 3: Distribution of distances (in km) to the nearest major road, by diagnosis type. Counts of villages are from within 3 standard deviational ellipses (SDEs) of all LP villages (referred to as the "study area" in text). In some cases, multiple patients came from the same village meaning that counts of villages will be smaller than counts of total patients. (Q1 and Q3 indicate the first and third quartiles, respectively).

	n	median distance in km (Q1 - Q3)
All	6416	5.4 (0.5 - 15.2)
Villages without study patient	5847	6.3 (0.8 - 16.1)
Villages with study patient	569	0.7 (0.1 - 4.1)
JEV	88	0.6 (0.1 - 8.0)
***Cryptococcus* spp.**	66	0.3 (0.1 - 1.4)
scrub typhus	31	0.6 (0.2 - 3.5)
Dengue virus	27	0.3 (0.1 - 1.1)
***Leptospirosis* spp.**	22	0.4 (0.1 - 1.9)
murine typhus	24	0.3 (0.1 - 2.2)

610 **Table 4**: Logistic regression and model adjusted odds ratios (AOR) for village level analysis of
611 LP villages

612

covariate	total	LP count	AOR (CI)
NDFI Q1	1604	68	reference group
NDFI Q2	1604	75	1.07 (0.73 - 1.56)
NDFI Q3	1604	130	**1.48 (1.03 - 2.16)**
NDFI Q4	1604	296	**2.21 (1.49 - 3.31)**
EVI Q1	1604	311	reference group
EVI Q2	1604	134	1.16 (0.86 - 1.57)
EVI Q3	1604	74	1.12 (0.76 - 1.66)
EVI Q4	1604	50	1.19 (0.74 - 1.91)
Village population			**2.22 (2.03 - 2.42)**
Elevation			**0.52 (0.42 - 0.63)**
Distance to major road			**0.68 (0.57 - 0.80)**

613

614 **Table 5**: Logistic regression and model adjusted odds ratios (AOR) for village level analysis of
615 JEV villages

covariate	total	JEV count	AOR (CI)
NDFI Q1	1604	18	reference group
NDFI Q2	1604	15	0.83 (0.38 - 1.76)
NDFI Q3	1604	20	1.11 (0.53 - 2.35)
NDFI Q4	1604	35	1.26 (0.54 - 2.95)
EVI Q1	1604	35	reference group
EVI Q2	1604	23	1.81 (0.87 - 3.76)
EVI Q3	1604	17	1.85 (0.77 - 4.46)
EVI Q4	1604	13	1.76 (0.63 - 4.93)
Village population			**1.74 (1.55 - 1.96)**
Elevation			**0.69 (0.46 - 0.97)**
Distance to major road			0.88 (0.62 - 1.20)

616

617

618

619

620

621 **Table 6:** Mixed effects logistic regression and model adjusted odds ratios (AOR) for individual
622 level analysis

			M1	M2	M3
covariate	**total**	**JEV count**	**AOR (CI)**	**AOR (CI)**	**AOR (CI)**
NDFI Q1	262	7	reference group	reference group	reference group
NDFI Q2	261	16	**2.91 (1.06 - 7.97)**	2.28 (0.86 - 6.01)	2.32 (0.87 - 6.19)
NDFI Q3	261	31	**2.73 (1.02 - 7.28)**	**2.75 (1.07 - 7.07)**	**2.98 (1.13 - 7.85)**
NDFI Q4	262	38	**3.41 (1.17 - 9.94)**	**3.12 (1.09 - 8.90)**	**3.06 (1.04 - 8.96)**
EVI Q1	262	8	reference group	reference group	reference group
EVI Q2	261	20	2.11 (0.84 - 5.28)	1.89 (0.76 - 4.74)	1.60 (0.63 - 4.04)
EVI Q3	261	24	2.04 (0.81 - 5.12)	1.65 (0.67 - 4.07)	1.33 (0.53 - 3.32)
EVI Q4	262	40	**4.19 (1.62 - 10.87)**	**3.44 (1.35 - 8.73)**	2.43 (0.91 - 6.46)
Jan - March	210	2	reference group	reference group	reference group
April - June	267	22	**5.12 (1.10 - 23.89)**	4.45 (0.95 - 20.76)	**5.05 (1.07 - 23.73)**
July - Sep	333	62	**8.72 (1.75 - 43.46)**	**6.35 (1.26 - 31.89)**	**7.40 (1.45 - 37.67)**
Oct - Dec	253	8	1.80 (0.35 - 9.25)	1.51 (0.29 - 7.81)	1.54 (0.29 - 8.17)
Year			**1.31 (1.03 - 1.68)**	**1.34 (1.05 - 1.72)**	1.27 (0.98 - 1.64)
0 through 4	208	13		reference group	reference group
5 through 14	150	37		**3.00 (1.46 - 6.18)**	**2.74 (1.31 - 5.69)**
15 through 24	192	28		1.74 (0.84 - 3.62)	1.37 (0.64 - 2.94)
25 through 34	186	10		0.66 (0.27 - 1.61)	0.61 (0.25 - 1.48)
35 through 44	133	4		**0.26 (0.07 - 0.96)**	**0.26 (0.07 - 0.97)**
45 plus	196	2		**0.11 (0.02 - 0.52)**	**0.10 (0.02 - 0.47)**
female	399	39		reference group	reference group
male	666	55		0.97 (0.60 - 1.58)	1.08 (0.66 - 1.79)
Village population					1.00 (0.77 - 1.29)
Elevation					**1.36 (1.11 - 1.66)**
Distance to major road					1.08 (0.88 - 1.32)

623

624

625

626

627

628

629

Figure 1: Spatial distributions of the home villages of study patients, for A: all study patients, B: study patients with JEV infections, and C: with cryptococcal infections, D: scrub typhus infections, E: with *dengue virus* infections, F: with leptospiral infections, and G: with murine typhus infections. SDDs and SDEs are weighted by case numbers, with some patients coming from the same village.

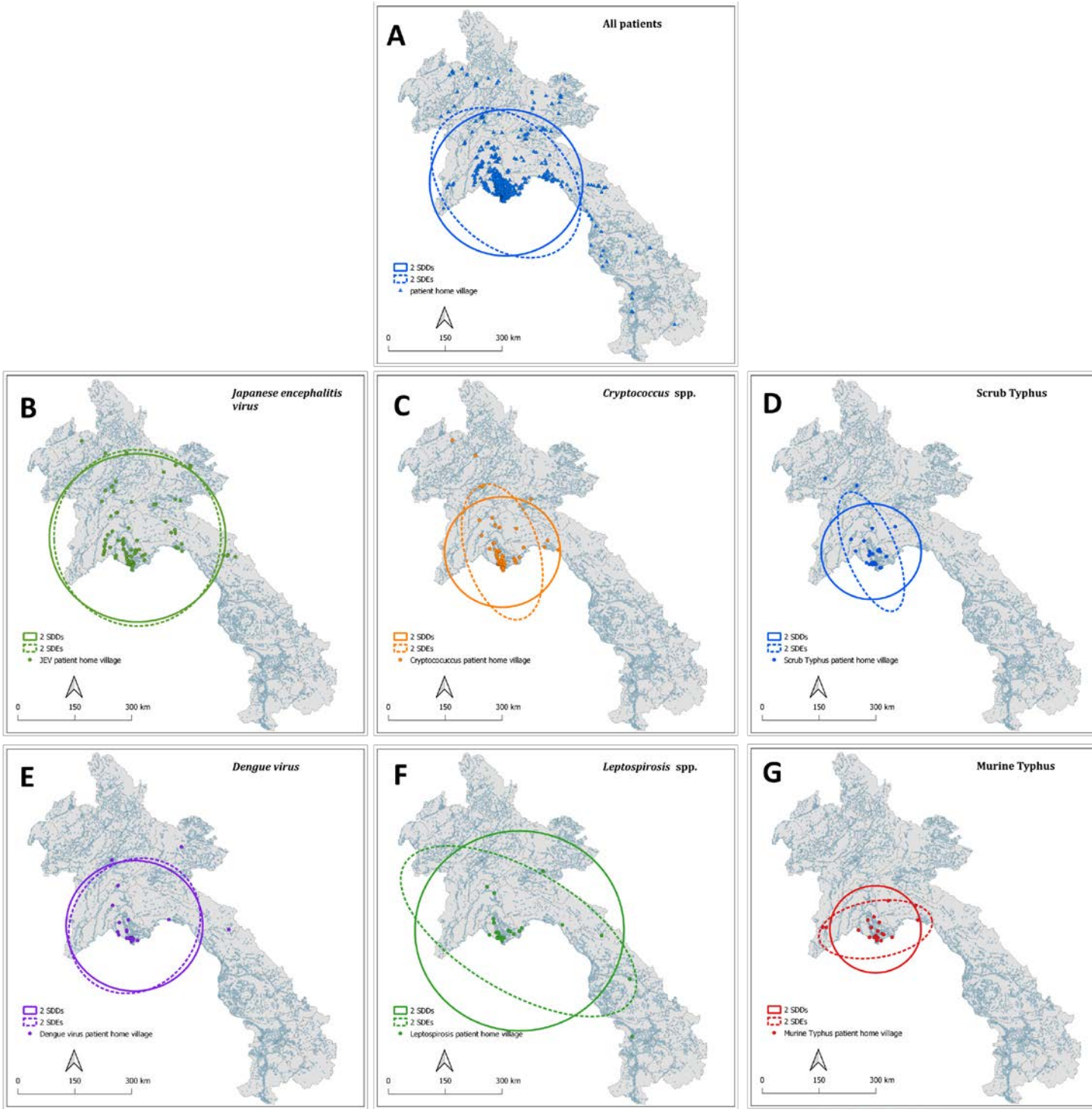

Figure 2: Environmental indices for villages with study patient homes for the duration of the study period (January 2003 through August 2011) for all study patient villages, non study patient villages in the study area, and for major diagnoses (JEV = Japanese Encephalitis virus; Crypto = cryptococcal infection; ST = scrub typhus; MT = murine typhus; dengue = Dengue virus; lepto = *Leptospira* spp. infection). Bar values are mean values and the error bars are 95% confidence intervals, using the t-distribution. NFI values here have a constant (0.25) added to them for visualization only.

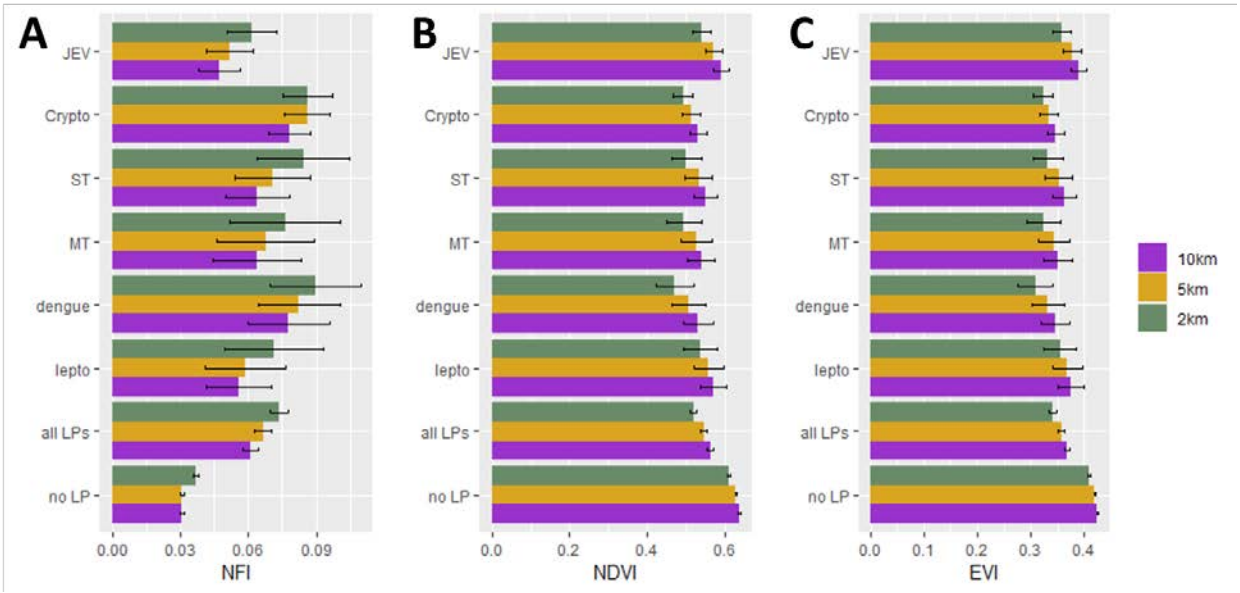

Figure 3: Environmental indices for study patients by major diagnosis and at different times leading up to the date of admission. JEV = Japanese Encephalitis virus; Crypto = cryptococcal infection; ST = scrub typhus; MT = murine typhus; dengue = *Dengue virus*; lepto = *Leptospira* spp. infection. Bar values are mean values and the error bars are 95% confidence intervals, using the t-distribution. NFI values here have a constant (0.25) added to them for visualization only.

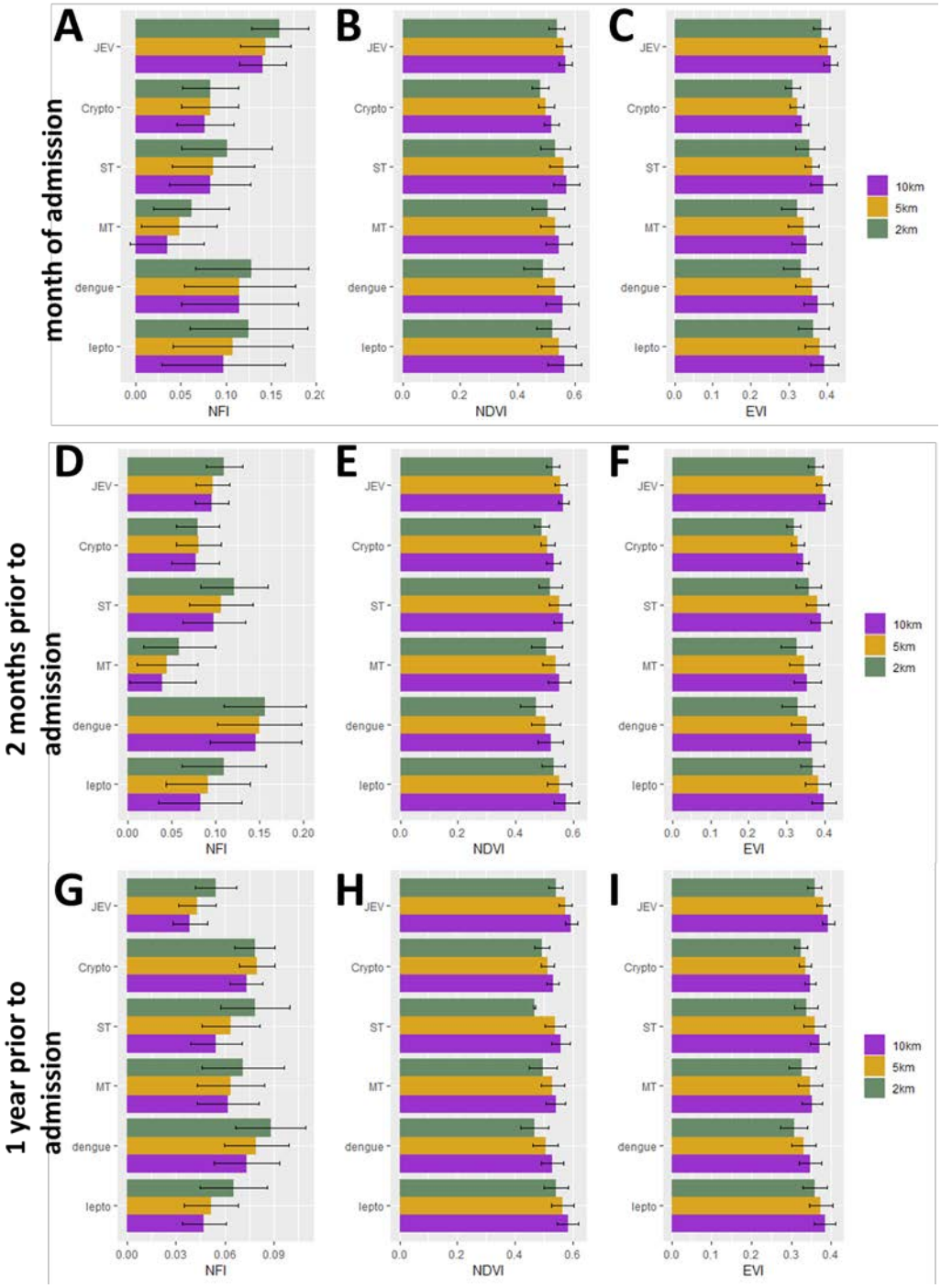

SUPPORTING MATERIALS

Supporting Materials I: Diagnosis of major infectious agents

A detailed report of the data collection and primary analysis can be found in [14]. Cerebrospinal fluid (CSF) was taken from all patients consenting to be included in this study (approximately 2.5 mL for children < 1yo; 3.5 mL for children 1 – 14yo; and 8 mL for patients ≥ 15yo). A venous blood sample was also taken on the same day as the lumbar puncture (approximately 5.5 mL for patients > 15yo; 10 mL for children 1 – 14yo; and 18.5 mL for patients ≥ 15yo). When possible follow-up serum samples were collected between 7 and 10 days post LP. All patient samples were analyzed using a panel of tests, including complete blood count; culture; biochemistry panel; and both serological and molecular assays for a range of fungi, parasites, viruses, and bacteria.

We considered sample size, natural history, and ecology of infections for selecting pathogens for this secondary analysis. Detections of the pathogens included in this analysis are as follows:

- *Japanese encephalitis virus* (JEV) infections were detected using ELISA IgM (Japanese Encephalitis/Dengue IgM Combo ELISA from Panbio) in CSF, and in serum at both admission and follow-up. Patients who were negative at admission but seropositive in a follow-up were classified as confirmed JEV infections. Some JEV infections were also diagnosed by culture or PCR.
- *Cryptococcus* spp. infections were detected using Indian ink stain of CSF; *Cryptococcus* Antigen Latex Agglutination Test with CSF (when HIV infection was suspected); and culture on Sabouraud agar when Indian ink test was positive or HIV infection was suspected.
- *Dengue virus* infections were detected using Hydrolysis probe real time RT-PCR [37] in CSF and serum; NS1 ELISA (Dengue Early ELISA from Panbio) in CSF and serum; and ELISA IgM (Japanese Encephalitis/Dengue IgM Combo ELISA from Panbio) in CSF, and in serum at both admission and follow-up (if negative at admission but seropositive in a follow-up).
- *Flavivirus* infections were detected using nested SYBR Green real-time RT-PCR in CSF and serum [38,39].
- *Rickettsia* spp. infections were detected using Hydrolysis probe RT-PCR in CSF [40,41]; Hydrolysis probe real time PCR and conventional PCR from buffy coat; and genetic sequencing.
- *R. typhi* and *Orientia tsutsugamushi* infections were detected using Hydrolysis probe real time PCR in CSF [40,41]; Hydrolysis probe real time PCR from buffy coat; and IgM and IgG assays from admission and follow-up serum (if there was a ≥ 4-fold rise in antibody at follow-up) [42].
- *Leptospira* spp. infections were detected using hydrolysis probe real-time PCR in CSF [43]; culturing of blood clot on EMJH medium; microscopic agglutination tests at

admission and follow-up (if there was a $\geq$ 4-fold rise in antibody at follow-up)[44]; and hydrolysis probe real time RT-PCR from buffy coat [43].

The final etiology was determined based on the panel of diagnostic tests, including direct detection of pathogens in CSF or blood, IgM in CSF, seroconversion, or a 4-fold increase in antibody titer between the date of admission and follow-up serum samples. When more than 1 pathogen was present, direct tests were prioritized over indirect tests and presence in the CSF was prioritized over presence in the blood.

Supporting Materials II: Spatial point patterns

The spatial distribution of villages from which study patients originated were indicated through maps of village locations, standard distance deviations (SDDs), and standard deviational ellipses (SDEs). Both SDDs and SDEs provide a visual representation of the central tendency and spread of points across a landscape [45,46]. SDEs also indicate potential anisotropy.

The SDD gives an indication of how points deviate from the mean center. The formula for the SDD is:

$$SDD = \sqrt{\frac{\sum_{i=1}^{n}(x_i - X_{MC})^2 + \sum_{i=1}^{n}(y_i - Y_{MC})^2}{n}}$$

where x_i and y_i are geographic references for point i;
$\{X_{MC}, Y_{MC}\}$ is the geometric mean center (MC) for the features.

The SDE differs from the SDD in that the X- and Y-axes are calculated separately and the orientation is not necessarily horizontal/vertical. The Y-axis is rotated clockwise until the sum of the squares of the distances between points (village locations) and axes are minimized. The angle is defined as:

$$\theta = arctan\left\{\frac{[\sum_{i=1}^{n}(x_i - X_{MC})^2 - \sum_{i=1}^{n}(y_i - Y_{MC})^2] + \sqrt{[\{(\sum_{i=1}^{n}(x_i - X_{MC})^2 - \sum_{i=1}^{n}(y_i - Y_{MC})^2)\}^2 + 4\{\sum_{i=1}^{n}(x_i}}{2\sum_{i=1}^{n}(x_i - X_{MC})(y_i - Y_{MC})}\right.$$

The standard deviation is then calculated along both the shifted X- and Y-axes:

$$s_X = \sqrt{\frac{\sum_{i=1}^{n}[(x_i - X_{MC})\cos\theta - (y_i - Y_{MC})\sin\theta]}{n}}$$

$$s_Y = \sqrt{\frac{\sum_{i=1}^{n}[(x_i - X_{MC})\sin\theta + (y_i - Y_{MC})\cos\theta]}{n}}$$

.

The output of these statistics is traditionally mapped as an ellipse; with 1, 2, or 3 standard deviations (roughly corresponding to 63, 98, or 99 % of all geographic points, respectively). Spatial point patterns that are isotropic will result in an SDE that is equal to the standard distance deviation (SDD), resulting in a circular map layer rather than an ellipse.

Both the SDD and SDE can be weighted (for example, if multiple cases come from a single location).

Supporting Materials III: Environmental Indices (EIs)

The photosynthetic components of vegetation (i.e. chlorophyll) absorb visible light, especially in the Red and Blue wavelengths. Conversely, most infrared radiation is reflected by healthy vegetation. The contrast between Red and near-infrared (NIR) responses therefore provides an estimate of healthy vegetation.

One common measure of landscape vegetation is the normalized difference vegetation index (NDVI [47]) which is frequently defined as:

$$NDVI = \frac{NIR - Red}{NIR + Red}$$

.

This simple measurement is sensitive to atmospheric effects and dense canopy structure [48]. While NIR can pass through multiple layers of canopy structure, Red typically cannot. In areas with high vegetation density NDVI quickly becomes saturated. An improved metric has been developed to account for these problems, referred to as the enhanced vegetation index (EVI [49]). This metric uses the difference between Red and Blue reflectances as an estimator of atmospheric influence level on the vegetation index. EVI is commonly specified as:

$$EVI = G\frac{NIR - Red}{NIR + C_1 Red - C_2 Blue + L}$$

; where L is the canopy background adjustment;
C_1 and C_2 are coefficients of an aerosol resistance term;
and G is a scaling factor.

A variety of similar indices have been proposed to measure water content, either within vegetation (i.e. measuring drought conditions or identifying areas that have been burned) or as surface water. In general, indices that use a combination of NIR and shortwave infrared responses (SWIR) have been proposed to measure within-vegetation water content whereas those that use a combination of visible spectral regions (VIS) and SWIR are usually proposed for identifying water bodies.

Almost all include a SWIR component because infrared in these wavelengths are well- absorbed by water (see [50], for example). Following Boschetti et al [51] we use the following normalized flooding index (NFI):

$$NFI = \frac{Red - SWIR2}{Red + SWIR2}$$

; where SWIR2 is shortwave infrared radiation 2 (~ 1640nm).

Supporting Materials IV: Statistical model selection

Formal multivariable analysis was conducted on both the village- and individual-level datasets. Small case numbers for mono-infections limited our multivariable analyses to an analysis of study patient home villages and comparison villages as well as the most commonly diagnosed infection: JEV. The village-level data were coded as a "1" or "0" based on whether or not the village was home to an study patient; and whether or not the village was home to an study patient diagnosed with JEV. The individual-level dataset was likewise coded with a "1" or "0" based on whether or not the individual was diagnosed with a JEV infection (all patients in the individual-level data had an LP).

We began with an exploratory multivariable analysis using generalized additive models (GAMs) with a binomial distribution (logistic GAMs). The use of GAMs allowed us to explore the potentially non-linear shape of the association between continuous environmental predictors (NDVI, EVI, and NFI) and the outcome variables and informed our final model selection and variable specification.

Our first GAMs included both NDVI and EVI, which are considered complimentary to each other [49]. The models showed a high degree of concurvity between these two covariates, almost no added benefit (from model fit statistics), and no detectable effect of the NDVI covariate. In subsequent models we therefore retained only EVI as a measure of vegetation.

Village-level GAMs began with village geographic (elevation, distance to nearest major road) and demographic (village population size) covariates. A second model was then specified including the environmental covariates at the 2km buffer size around each village. Subsequent models tested larger buffer sizes (5km and 10km), investigating overall model fit using the Akaike Information Criterion (AIC) and the explained deviance. The smoothed functions were chosen using restricted maximum likelihood (REML).

The village-level GAM for all study patients (that is, all patients who had an LP regardless of diagnosis) showed statistically significant contributions from NFI, EVI, village population, distance to the nearest major road, and elevation. The effects of NFI, EVI, and village population were positive while the effects for distance to the nearest major road and elevation were negative. The effects for NFI, EVI, village population, and elevation all appeared curvilinear. The village level model for JEV villages (villages from which LP patients who were diagnosed with JEV came) indicated that only village population was a significant predictor, with a curvilinear effect.

Individual-level models began with village- (village population, elevation, distance to the nearest major road) and individual- (age, gender, admission quarter and year) level variables. Environmental variables were first added at the 2km buffer size and for the year prior to admission. Subsequent models tested larger buffer sizes until the AIC was minimized. The 10km buffer appeared to provide the best model fit. The temporal resolution was then varied at the

10km buffer size, beginning with 1 year mean prior to admission, then 2 months mean prior to admission, and finally within the same month as admission. The best fitting model appeared to be the 10km buffer and measures from the same month as admission.

Both NFI and EVI show seasonal variations and calendar month is a strong predictor of NFI. In order to account for concurvity in the GAMs and collinearity in the subsequent logistic generalized linear models, we transformed the environmental variables to quartiles for subsequent models. This transformation allows for easy interpretation of covariate effects, allows for non-linear associations between the covariate and the outcome of interest, and allows the model to simultaneously address both the seasonality in cases (especially JEV) and the apparent associations with surface water (NFI).

All other continuous variables were centered on their means and standardized by their standard deviations.

The final village-level model was a logistic regression and the final individual-level model was a mixed effects logistic regression, with a random intercept for village, both using these transformed and standardized variables.

SUPPORTING FIGURES

Supporting Figure 1: Diagram of data processing and aggregation. Four different data sources are used (indicated by boxes with dashed lines). Two main datasets are created from the combined sources (indicated by boxes shaded in grey): an individual-level dataset (one row per patient) and a village-level dataset (one row per village). NDVI indicates the normalized differential vegetation index, EVI indicates the enhanced vegetation index, and NFI indicates the normalized flooding index.

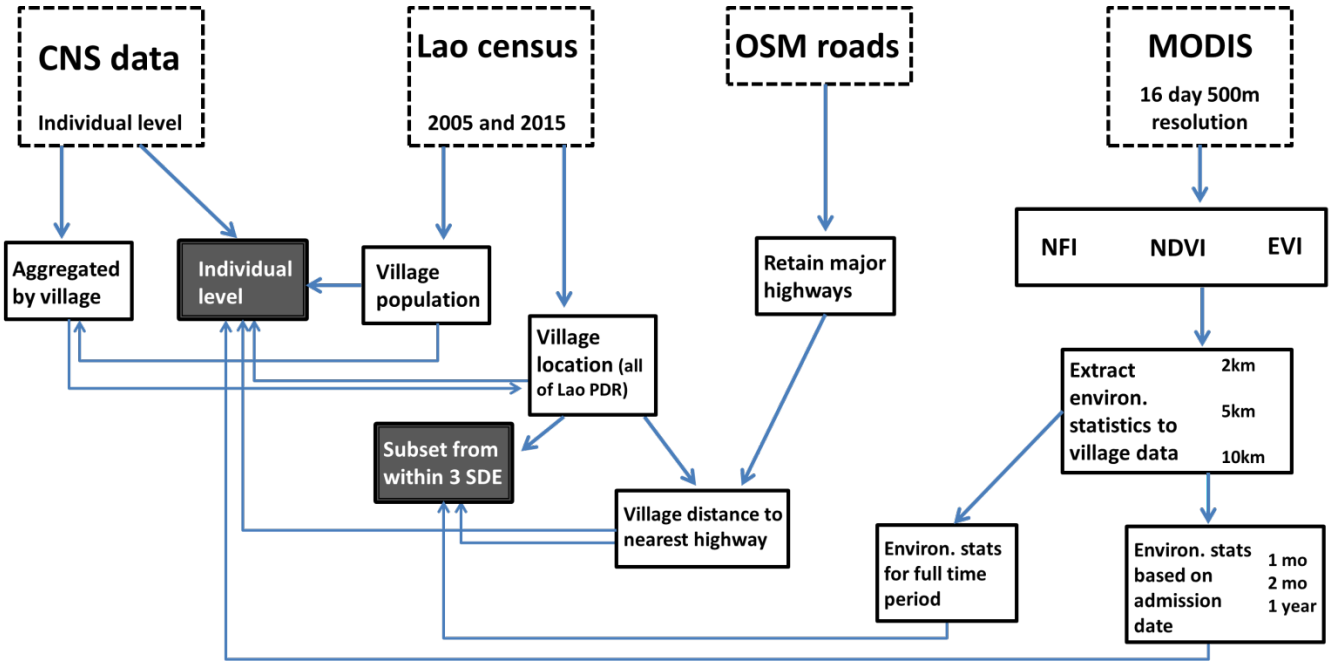

Supporting Figure 2: Subset of villages selected for village level analysis. A standard deviational ellipse ((SDE) with 3 standard deviations) was drawn around the home villages of all LP patients. All villages within that SDE were selected for the village level analysis.

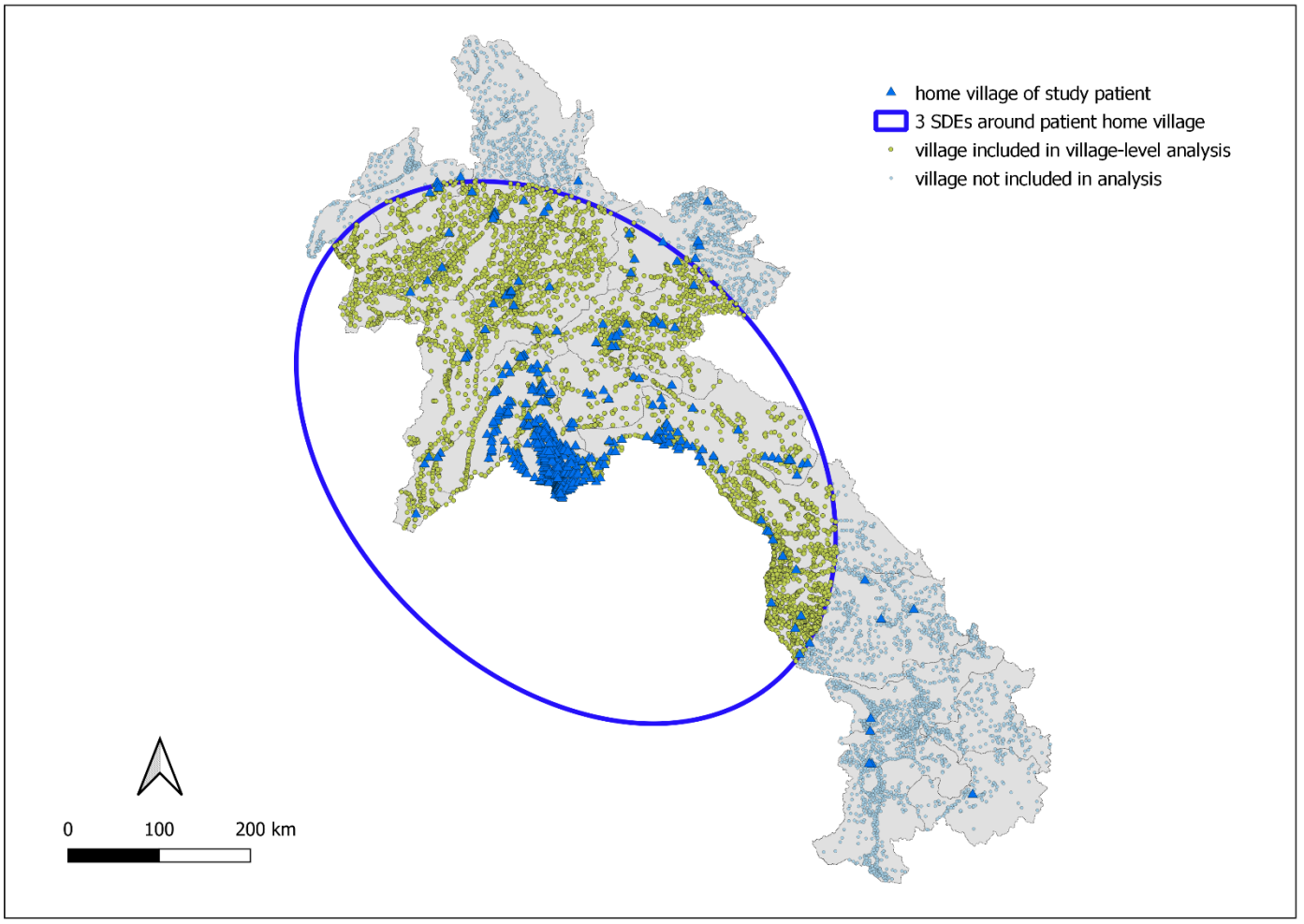

930 **Supporting Figure 3**: Major roads (dark black lines) downloaded from OpenStreetMaps (2017)
931 for use in calculating the Euclidian distance from each village to the nearest major road. Roads
932 included "primary", "secondary", and all major connecting roads.

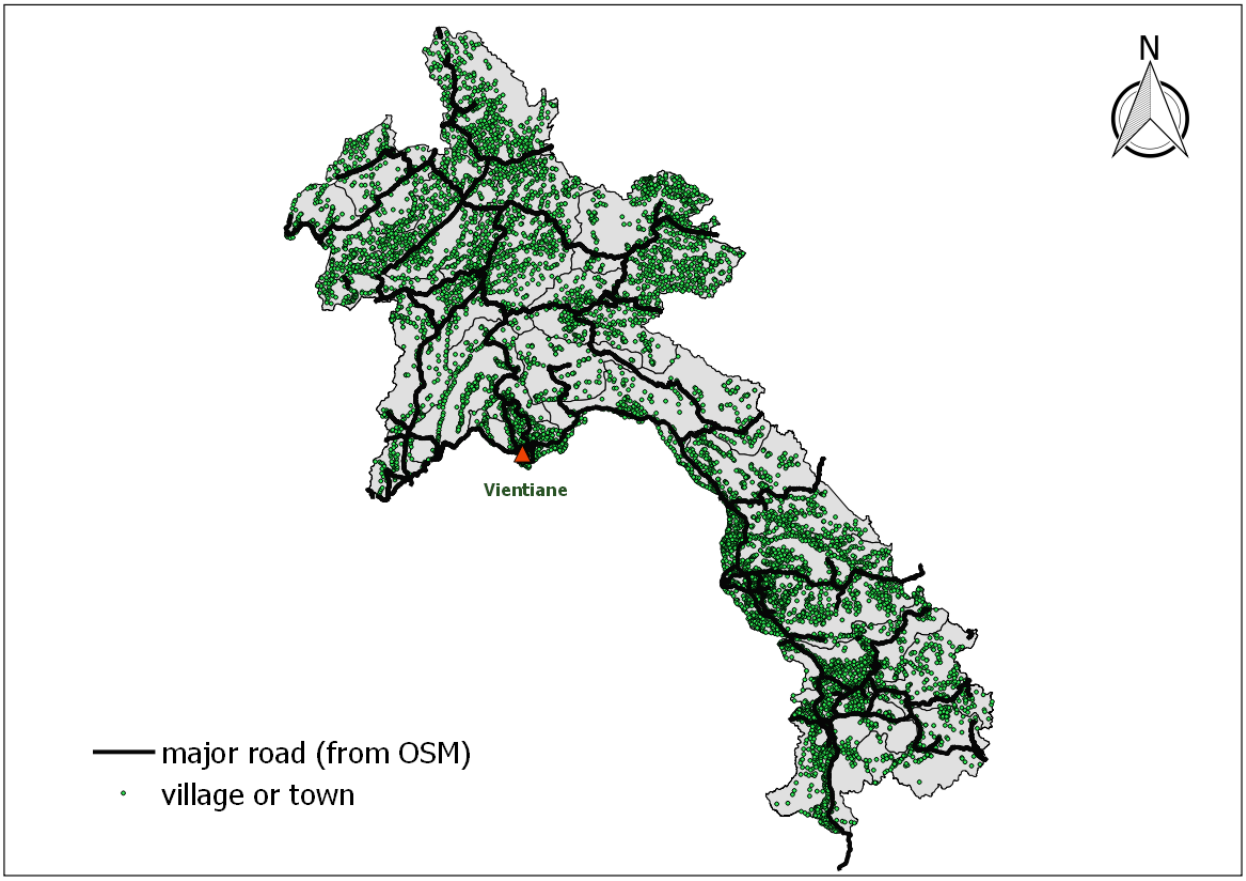

933
934
935
936
937
938
939
940
941
942
943

944 **Supporting Figure 4:** Mean village population (and 95% CI) by diagnosis

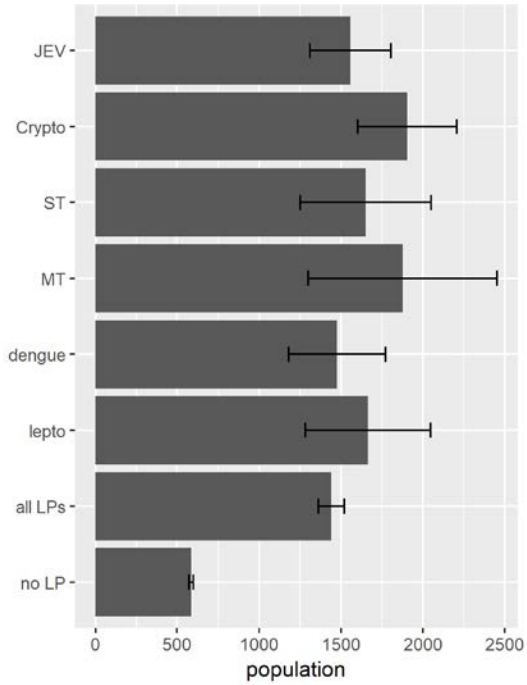

945

946

947 **Supporting Figure 5:** Mean village elevation (and 95% CI) by LP diagnosis

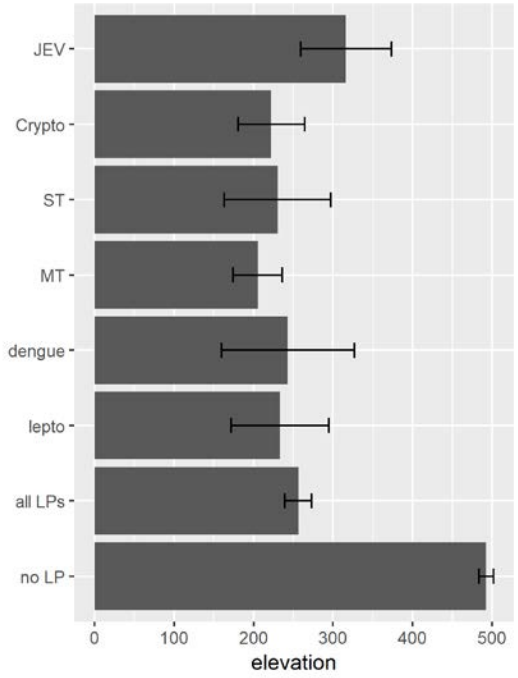

948

949